

# Hardware Impairments in Millimeter Wave Communications using OFDM and SC-FDE

Meng Wu, Dirk Wübben, Armin Dekorsy  
University of Bremen, Bremen, Germany

Email: {wu, wuebben, dekorsy}@ant.uni-bremen.de

Paolo Baracca, Volker Braun, Hardy Halbauer  
Bell Labs, Nokia, Germany

Email: {paolo.baracca, volker.braun, hardy.halbauer}@nokia.com

**Abstract**—Millimeter wave (mmWave) communications are recognized as a key technology in 5G architecture by achieving highly boosted data rates due to the large available bandwidth. For proper mmWave air interface design, the impact of hardware impairments leading to performance degradations have to be considered adequately in practical systems. In this paper, we study the hardware aspects phase noise, non-linear power amplifiers, IQ imbalance, and analog-to-digital converter (ADC) resolution using appropriate models at mmWave frequency and evaluate the performance in an outdoor urban mmWave scenario. The respective influence on two air interfaces, namely, orthogonal frequency division multiplexing (OFDM) and single-carrier frequency domain equalization (SC-FDE), are analyzed and compared. It is shown that SC-FDE is much more robust against impairments from non-linear power amplifiers, IQ imbalance and ADC resolution than OFDM for a typical mmWave system configuration. Although this less robustness of OFDM systems is compensated by channel coding significantly, SC-FDE with minimum mean square error equalization can still outperform OFDM in some coded cases.

## I. INTRODUCTION

For practical system designs of mmWave access at high frequencies between 3GHz and 300GHz, hardware impairments from the radio frequency (RF) chains should be considered adequately for realistic performance evaluations. In [1], several hardware aspects are described to facilitate 60 GHz simulations intended for wireless personal area networks (WPAN), including phase noise (PN), non-linear power amplifiers (NPA), and IQ imbalance. Proper modeling of these imperfections at mmWave range is of special importance and is required to study the resulting performance degradation in different channel scenarios. These aspects are investigated in additive white Gaussian noise (AWGN) channels at 60 GHz for orthogonal frequency division multiplexing (OFDM) and single-carrier frequency domain equalization (SC-FDE) systems in [2]. Similar investigations and comparisons are presented for an indoor WPAN environment in [3]. In this paper, we consider an outdoor mmWave scenario with a recently proposed 3D channel model [4] using a sectorized beamforming model [5]. Employing this mmWave channel with beamforming we performed an initial comparison of OFDM and SC-FDE assuming perfect hardware configurations in [6]. Here, we extend this analysis by incorporating hardware impairments and study the corresponding impact on both air interfaces. The numerical results give insights into practical system design for outdoor mmWave communications.

The remainder of this paper is organized as follows. The system setup including the employed mmWave channel model as well as parametrization for link level simulations is introduced in Section II. The impact of hardware impairments, namely, phase noise, non-linear power amplifier, IQ imbalance, and analog-to-digital converter (ADC) resolution, are analyzed in Section III, Section IV, Section V, and Section VI in succession. Performance evaluations that highlight the comparison between OFDM and SC-FDE transmissions in both uncoded and coded systems with the respective impairment are also presented in detail. Section VII concludes this paper.

## II. SYSTEM SETUP

A single-stream mmWave communication system is considered in outdoor urban non line of sight (NLOS) scenarios using the channel model proposed in [4] at 73 GHz. To compensate the large path-loss at mmWave range, a sectorized beamforming model [5] is employed and built on top of the channel, as described in [6]. Specifically, we adopt a beam with a constant gain within a given beamwidth  $\theta$ . This beam is steered in the direction leading to the highest receive signal to noise ratio (SNR). Note that narrower beam yields less frequency selectivity of the mmWave channel [6]. Without hardware impairments, it is well known that SC-FDE with minimum mean square error (MMSE) equalization outperforms OFDM in uncoded systems whereas OFDM becomes superior to SC-FDE applying coding [7]. However, due to reduced peak to average power ratio (PAPR), SC-FDE might be beneficial over OFDM considering hardware impairments, as discussed in this work.

For performance evaluation, the numerology for OFDM and SC-FDE transmissions follows those in the METIS project [8]. Each data frame employs  $N_C = 2048$  subcarriers and 4-QAM modulation with a subcarrier spacing of  $\Delta f = 720$  kHz if not otherwise stated. The length of cyclic prefix (CP) is set to be  $1/8$  of the data frame, which is sufficient to avoid interference from the previous frame when employing a beamwidth of  $\theta = 7^\circ$  in the beamforming model [6]. In coded systems, an LDPC code of rate  $R_C = 0.5$  is used to encode each data frame individually with a maximum of 100 iterations for decoding. The SNR is defined as  $E_b/N_0 = 1/(\log_2(M)R_C\sigma_n^2)$  to include to impact of modulation alphabet  $M$ , the code rate  $R_C$ , and the noise variance  $\sigma_n^2$ .

### III. PHASE NOISE

In communication systems, mixers are applied for signal up-conversion at the transmitter and down-conversion at the receiver using local oscillators to generate carrier signals operating at the prescribed carrier frequency. However, due to random deviation of the output signal frequency around the carrier, it is infeasible that both oscillators at the transmitter and the receiver operate exactly at the same carrier frequency. Such a mismatch leads to signal distortion in form of inter-carrier interference (ICI) and inter-symbol interference (ISI) for OFDM and SC-FDE transmissions, respectively. In order to capture this effect, the instability of carrier signal generators is depicted by the phase noise (PN) since the frequency offset yields a random phase difference for the time domain samples. Thus, an appropriate PN model is required to consider this hardware impairment for performance evaluations.

In [9], a typical PN model based on its power spectral density (PSD) is presented for performance evaluation in IEEE P802.11 WLAN standardization. This model can be viewed as a high-pass filter with PSD given by

$$\text{PSD}(f) = \delta \cdot \frac{1 + (f/f_z)^2}{1 + (f/f_p)^2}, \quad (1)$$

where  $\delta$  represents the low frequency phase noise level. The pole and zero frequencies are denoted by  $f_p$  and  $f_z$ , which indicate the low and high frequency transitions, respectively. Assuming typical values  $f_p = 1$  MHz and  $f_z = 100$  MHz for 60 GHz PN modeling [9], the one-sided PSD with different  $\delta$  values is shown in Fig. 1. As can be observed, the noise level transits from  $\delta$  at low frequencies to a noise floor  $\delta - 40$  dB at high frequencies. Note that this 40 dB gap can be easily obtained by forcing  $f \rightarrow \infty$  in (1) with the given  $f_p$  and  $f_z$  values above.

As an alternative, a PN model using another PSD definition is given in [10] being consistent with the theoretical background in view of correlation functions. The PSD with a logarithmic decay is given by

$$\text{PSD}(f) = 10^{-c} + \begin{cases} 10^{-a} & |f| \leq f_l \\ 10^{-a}(f/f_l)^{-b} & f > f_l \\ 10^{-a}(-f/f_l)^{-b} & f < -f_l \end{cases} \quad (2)$$

with fitting parameters  $a, b, c$  and the low transition frequency  $f_l$  equivalent to  $f_p$  in (1) for the IEEE model. For coherence, the parameters in this PN model are selected to fit best with the IEEE model [11]. The resulting PSD is again shown in Fig. 1 with different  $\delta$  values, where both PN models coincide well except for a slight PSD discrepancy around the low frequency transition. Specifically, a hard transit is observed for the model [10]. In the sequel, we adopt the PSD model (2) for performance evaluation without special preference to either model.

For system evaluation with PN using the given PSD model (2), a Gaussian noise sequence is firstly generated. By fast Fourier transform (FFT) its frequency domain representation is achieved, multiplied with the PSD samples and subsequently

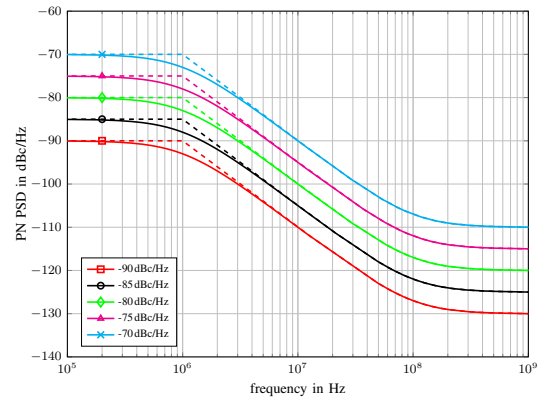


Fig. 1: One-sided PSD characteristics for PN modeling with different low frequency phase noise level  $\delta$ , IEEE model (1) (—) and logarithmic decay model (2) (---).

transformed back to time domain by inverse fast Fourier transform (IFFT) yielding the PN sequence  $\varphi$ . By element-wise multiplication of the time samples of the transmit or the receive signal with  $e^{j\varphi}$  the PN is introduced. This procedure for incorporating PN is shown in Fig. 2. It is noted that the PN needs to be considered at both transmitter and receiver side.

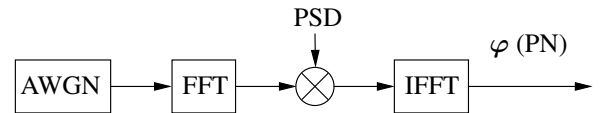


Fig. 2: Block diagram for PN generation using given PSD.

The error rate performance considering PN with varying  $\delta$  is shown in Fig. 3 and Fig. 4 for OFDM and SC-FDE with MMSE equalization, respectively. Both uncoded bit error rates (BER) and coded frame error rates (FER) are presented, where a frame error occurs when at least one bit is in error over the whole frame. As expected for the ideal case without PN, SC-FDE outperforms OFDM for uncoded transmission and the performance is comparable for coded transmission [6]. In case of PN, the system performance degrades in general, where more severe PN is indicated by a larger low frequency phase noise level  $\delta$ . For uncoded systems, the performance suffers only slightly at high SNR with  $\delta = -90$  dBc/Hz. Interestingly, by comparing Fig. 3(a) and Fig. 4(a) it can be observed that OFDM is more robust against PN than SC-FDE. Specifically, OFDM even outperforms SC-FDE with PN of  $\delta = -80$  dBc/Hz or more at high SNR. This can be explained by comparing the signal constellations after equalization [12], as shown in Fig. 5 for OFDM and SC-FDE at  $E_b/N_0 = 36$  dB. Therein, the ICI for OFDM and the ISI for SC-FDE originated from PN yield circles and arcs, respectively, indicating that OFDM corresponds to more equalized signal samples that are closer to the noise-free constellation points than SC-FDE and thus is less sensitive to PN.

In coded systems, the impairment from PN is mitigated

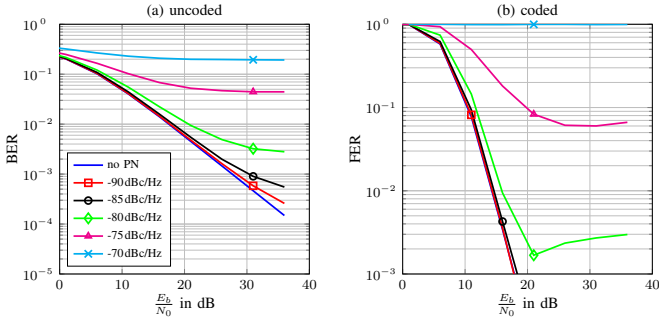


Fig. 3: Error rate for OFDM with PN of different low frequency phase noise level  $\delta$ , (a) for uncoded BER and (b) for coded FER.

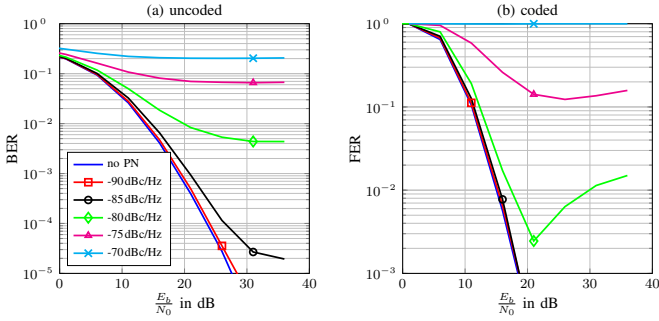


Fig. 4: Error rate for SC-FDE with PN of different low frequency phase noise level  $\delta$ , (a) for uncoded BER and (b) for coded FER.

tremendously by channel coding for both OFDM and SC-FDE systems. For instance, PN with  $\delta = -85$  dBc/Hz already approaches the ideal case also in the high SNR region. Furthermore, OFDM achieves much lower error floor than SC-FDE at, e.g.,  $\delta = -80$  dBc/Hz since channel coding is able to better exploit the channel frequency selectivity for OFDM. Note that the FER in this case even raises with growing SNR. This is because the soft demapper that produces bit-level log-likelihood ratios (LLRs) for channel decoding assumes Gaussian interference and noise. When the ICI and ISI power caused by PN become dominant compared to the AWGN variance as the SNR increases, the LLRs may not be calculated precisely, thus leading to degraded performance.

#### IV. NON-LINEAR POWER AMPLIFIERS

In case of linear power amplifiers (LPA), the transmit signals would only be scaled linearly without distortion. However, in practice each amplifier shows a non-linear behaviour, e.g., input signals of large amplitude are clipped. For modeling of such non-linear characteristics, the modified Rapp model [1], [13] is commonly used to describe the input-output characteristics of the NPA. Denoting  $x_{\text{in}}$  the input voltage level of the power amplifier, the output voltage level  $x_{\text{out}}$  is described by the amplitude modulation to amplitude modulation (AM-AM)

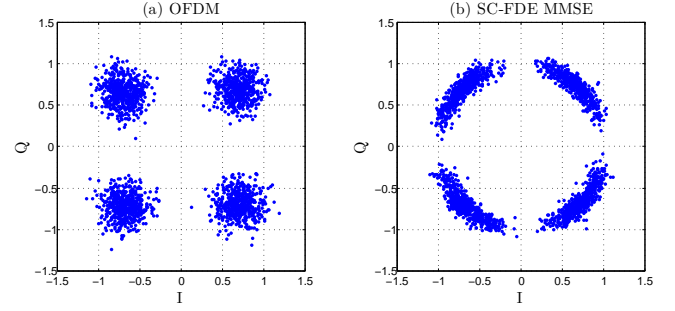


Fig. 5: Equalized signal constellation with PN of  $\delta = -80$  dBc/Hz and  $E_b/N_0 = 36$  dB, (a) for OFDM and (b) for SC-FDE.

characteristic

$$x_{\text{out}} = F_{\text{AM-AM}}(x_{\text{in}}) = Gx_{\text{in}} / \left( 1 + \left( \frac{Gx_{\text{in}}}{V_{\text{sat}}} \right)^{2p} \right)^{\frac{1}{2p}} \quad (3)$$

and the phase change  $\psi$  between input and output signals is modeled by the amplitude modulation to phase modulation (AM-PM) characteristics

$$\psi = F_{\text{AM-PM}}(x_{\text{in}}) = Ax_{\text{in}}^q / \left( 1 + \left( \frac{x_{\text{in}}}{B} \right)^q \right). \quad (4)$$

The gain of the power amplifier  $G$ , the saturation voltage level  $V_{\text{sat}}$ , the smoothness factor  $p$  controlling the curvature of the AM-AM saturation transfer behavior and the fitting parameters  $A$ ,  $B$ ,  $q$ , are set to  $G = 16$ ,  $V_{\text{sat}} = 1.9$ ,  $p = 1.1$ ,  $A = -345$ ,  $B = 0.17$  and  $q = 4$  following [14] for performance evaluation at 60 GHz in the WPAN standardization. Using these numbers, the AM-AM and AM-PM characteristics are plotted in Fig. 6. It can be observed that linear behavior as well as negligible phase change is only achieved with small input signal voltage. As the input voltage level increases, the output voltage level saturates at  $V_{\text{sat}} = 1.9$ , whereas the phase change converges to no more than  $-0.3$  in rad (approximately  $-17^\circ$ ).

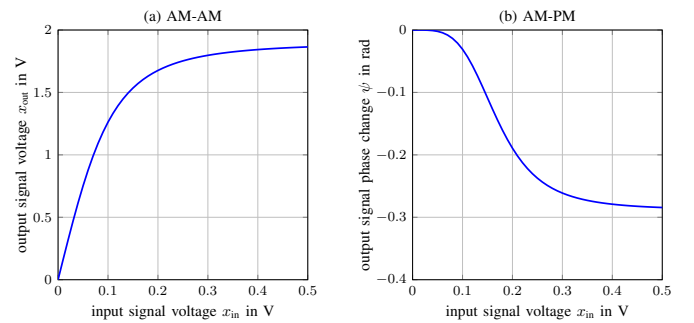


Fig. 6: Input-output characteristics for NPA using modified Rapp model, (a) for AM-AM and (b) for AM-PM.

In order to avoid non-linear distortions such as signal clipping and phase rotation, the power amplifier should be operated in the linear zone. For this purpose, the input signal power needs to be backed off to keep the signal within the

linear zone at the expense of lower power efficiency. This is especially important for input signals with a high PAPR since the operating point of the power amplifier changes. To quantify the amount of power that is backed off for the NPA, the output back-off (OBO) power ratio in dB is defined as

$$\text{OBO} = 10 \log_{10} \frac{P_{\text{sat}}}{P_{\text{out}}}, \quad (5)$$

where  $P_{\text{sat}}$  and  $P_{\text{out}}$  represent the saturation output power and the average output power emitted from the NPA. Larger OBO leads to improved linearity but a lower receive SNR [15].

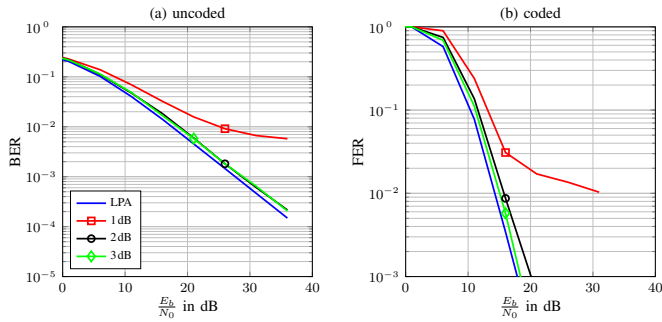


Fig. 7: Error rate for OFDM using 4-QAM and NPA with different OBO, (a) for uncoded BER and (b) for coded FER.

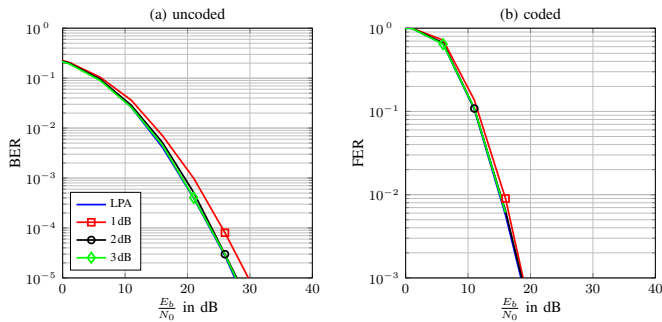


Fig. 8: Error rate for SC-FDE using 4-QAM and NPA with different OBO, (a) for uncoded BER and (b) for coded FER.

In Fig. 7 and Fig. 8, both uncoded BER and coded FER for OFDM and SC-FDE using 4-QAM with NPA parameters from [14] and different OBO values are presented, respectively. The power inefficiency caused by power back-off is not included here. As can be observed, larger OBO leads to improved performance in general. SC-FDE is much more robust against signal distortions from NPA than OFDM. For example, in uncoded cases with  $\text{OBO} = 1$  dB, SC-FDE leads only to a small performance degradation compared to the ideal case (LPA), whereas OFDM encounters an error floor. This confirms that OFDM is very sensitive to NPA due to higher PAPR resulting in a large dynamic range of the transmit signal envelope. Additionally, although having constant signal envelope for 4-QAM, SC-FDE still requires  $\text{OBO} = 2$  dB to reach the performance using LPA because of the AM-PM distortion shown in Fig. 6. In case of coded systems, the impairment from

NPA is mitigated to some extent. Exemplarily, as observed in Fig. 8(b) for SC-FDE,  $\text{OBO} = 1$  dB already approaches the ideal case (LPA) with only a slight performance loss.

Subsequently, performance results indicating the impact of NPA for larger modulation schemes are presented. The uncoded BER for OFDM and SC-FDE are plotted in Fig. 9 and Fig. 10 for 16-QAM and 64-QAM, respectively. Again, the robustness of SC-FDE against NPA over OFDM is confirmed. Furthermore, using the same OBO is not sufficient to achieve reasonable performance for higher modulation alphabets. Thus, larger OBO values are required to approach the benchmark performance of LPA, however, by sacrificing the power efficiency.

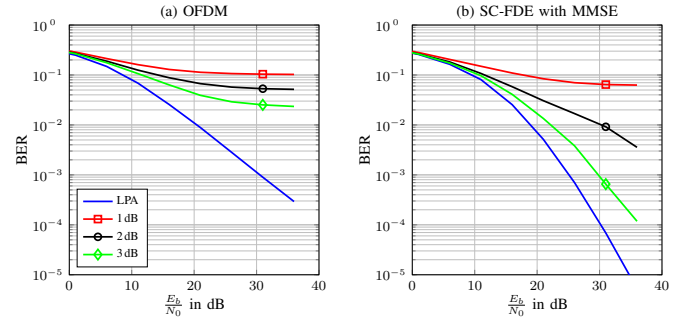


Fig. 9: Uncoded BER for (a) OFDM and (b) SC-FDE using 16-QAM and NPA with different OBO.

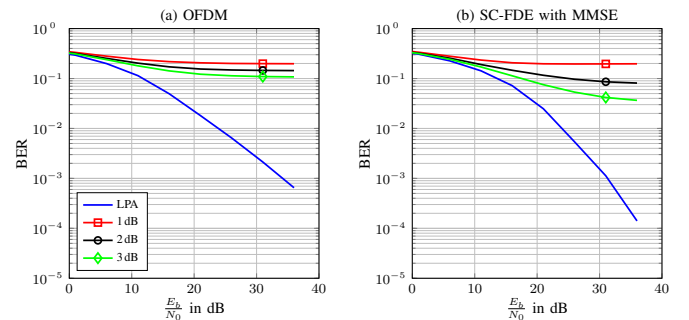


Fig. 10: Uncoded BER for (a) OFDM and (b) SC-FDE using 64-QAM and NPA with different OBO.

The previous results on NPA do not include the power loss caused by OBO. Although larger OBO forces the operating point of the NPA back to the linear zone, thus reducing non-linear distortions, this also leads to decreased receive SNR which in turn reduces estimation performance. Considering this trade-off, there must exist an optimal OBO value that reaches a compromise between both counterparts to achieve the best performance [15]. To this end, a numerical search is initiated by simulating over a sequence of successive OBO values with a fixed  $E_b/N_0 + \text{OBO}$ . In this way, the power loss from OBO is included in the analysis as a higher OBO value corresponds to a smaller receive SNR.

For varying OBO Fig. 11, Fig. 12, and Fig. 13 indicate the impact on the uncoded BER and the coded FER of OFDM

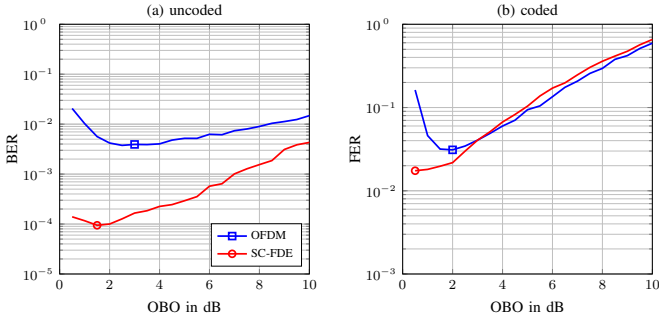


Fig. 11: Error rate for OFDM and SC-FDE using 4-QAM and NPA with different OBO at fixed  $E_b/N_0 + \text{OBO}$ , (a) for uncoded BER at  $E_b/N_0 + \text{OBO} = 26$  dB and (b) for coded FER at  $E_b/N_0 + \text{OBO} = 16$  dB.

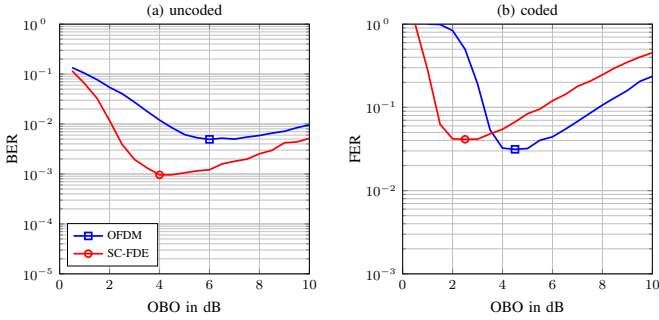


Fig. 12: Error rate for OFDM and SC-FDE using 16-QAM and NPA with different OBO at fixed  $E_b/N_0 + \text{OBO}$ , (a) for uncoded BER at  $E_b/N_0 + \text{OBO} = 31$  dB and (b) for coded FER at  $E_b/N_0 + \text{OBO} = 21$  dB.

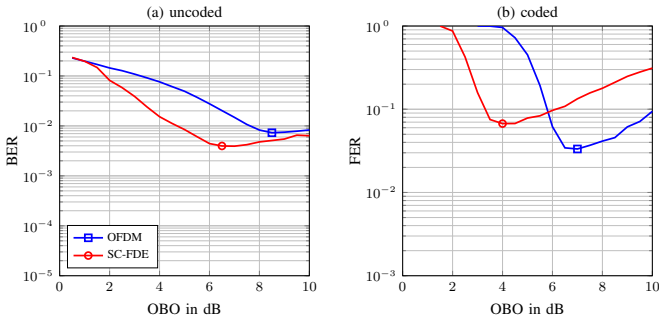


Fig. 13: Error rate for OFDM and SC-FDE using 64-QAM and NPA with different OBO at fixed  $E_b/N_0 + \text{OBO}$ , (a) for uncoded BER at  $E_b/N_0 + \text{OBO} = 36$  dB and (b) for coded FER at  $E_b/N_0 + \text{OBO} = 26$  dB.

and SC-FDE for 4-QAM, 16-QAM and 64-QAM modulations, respectively. By markers, the optimum OBO for the fixed  $E_b/N_0 + \text{OBO}$  are indicated. It can be observed, that SC-FDE accounts for smaller optimal OBO values compared to OFDM and the optimum OBO is reduced for coded systems. Moreover, higher modulation alphabets requires larger optimal OBO values. These conclusions coincide with those indicated from the previous results without considering the power loss

		4-QAM	16-QAM	64-QAM
uncoded	OFDM	3 dB	6 dB	8.5 dB
	SC-FDE	1.5 dB	4 dB	6.5 dB
coded	OFDM	2 dB	4.5 dB	7 dB
	SC-FDE	0.5 dB	2.5 dB	4 dB

TABLE I: Optimal OBO in dB for OFDM and SC-FDE using different modulation alphabets with respect to uncoded BER and coded FER.

by OBO. For the sake of complete comparisons, the optimal OBO values  $\text{OBO}_{\text{opt}}$  read from Fig. 11, Fig. 12 and Fig. 13 in different scenarios are summarized in Tab. I.

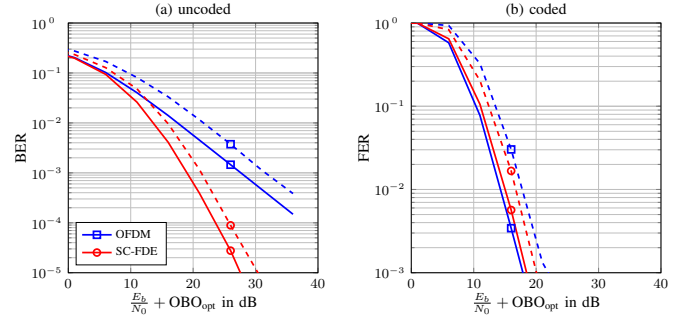


Fig. 14: Error rate for OFDM and SC-FDE using 4-QAM, LPA (—) or NPA with optimal OBO (---), (a) for uncoded BER and (b) for coded FER.

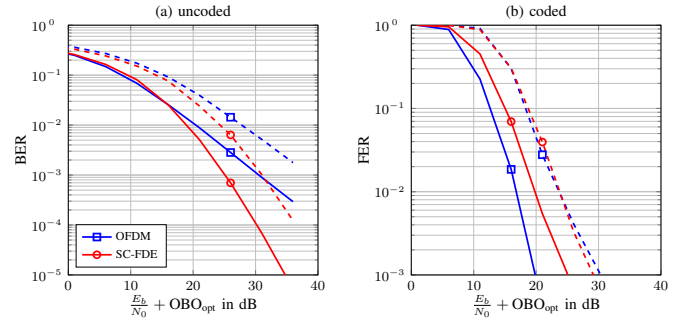


Fig. 15: Error rate for OFDM and SC-FDE using 16-QAM, LPA (—) or NPA with optimal OBO (---), (a) for uncoded BER and (b) for coded FER.

Using these optimal OBO values and assuming they are consistent with the SNRs, the performances of OFDM and SC-FDE are presented with respect to  $E_b/N_0 + \text{OBO}_{\text{opt}}$  using 4-QAM, 16-QAM and 64-QAM in Fig. 14, Fig. 15 and Fig. 16, respectively. Note that  $\text{OBO}_{\text{opt}}$  refers to the optimal OBO value that is different in the x-axis in the respective scenarios. This allows for a fair comparison of OFDM and SC-FDE as the loss from power back-off under optimal OBO values is considered. It is observed, that the performance loss caused by NPA compared to the ideal case (i.e. with LPA) is enlarged for higher modulation alphabets. Comparing the results with NPA, SC-FDE is superior to OFDM in all uncoded cases with the

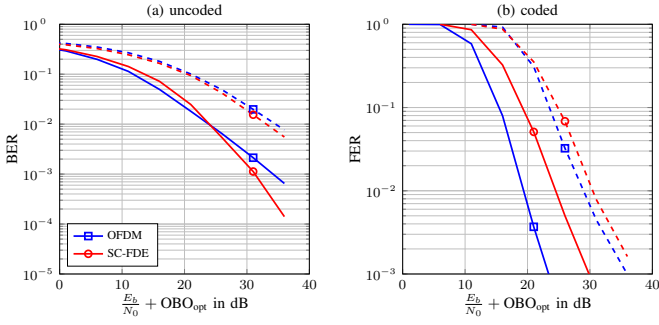


Fig. 16: Error rate for OFDM and SC-FDE using 64-QAM, LPA (—) or NPA with optimal OBO (---), (a) for uncoded BER and (b) for coded FER.

gain decreasing as the modulation alphabet grows. It should be noted, that SC-FDE also outperforms OFDM for coded transmission by more than 1 dB in case of 4-QAM, although OFDM is slightly better in the ideal case with LPA. This indicates that practical issues from hardware impairments may alter the preferable air interface when designing the system.

## V. IQ IMBALANCE

In quadrature modulators and demodulators, the front-end components may not completely respect the orthogonality between the in-phase (I) and quadrature (Q) signal branches, resulting in IQ imbalance characterized by an amplitude offset  $\epsilon$  and a phase offset  $\Delta\phi$ . In [16], both amplitude and phase mismatches are assumed to be symmetric between the real part and the imaginary part of the signal. We follow this model here, so that the input signal  $x_{\text{in}}$  of either a modulator at the transmitter or a demodulator at the receiver suffering from IQ imbalance yields the output signal

$$x_{\text{out}} = (\cos \Delta\phi + j\epsilon \sin \Delta\phi) x_{\text{in}} + (\epsilon \cos \Delta\phi - j \sin \Delta\phi) x_{\text{in}}^* \quad (6a)$$

$$= \alpha x_{\text{in}} + \beta x_{\text{in}}^* . \quad (6b)$$

This implies that the signal  $x_{\text{in}}$  is interfered with its own complex conjugate  $x_{\text{in}}^*$ . The desired signal and the interference signal are weighted by  $\alpha$  and  $\beta$  given by

$$\alpha = \cos \Delta\phi + j\epsilon \sin \Delta\phi \quad (7a)$$

$$\beta = \epsilon \cos \Delta\phi - j \sin \Delta\phi . \quad (7b)$$

Obviously, smaller amplitude and phase mismatches yield larger  $|\alpha|$  and smaller  $|\beta|$ , and therefore, the impairment from IQ imbalance is less severe. The interference from  $x_{\text{in}}^*$  causes attenuation and rotation of the original signal  $x_{\text{in}}$ , leading to ICI for OFDM and ISI for SC-FDE transmissions [17].

As indicated above, both modulator and demodulator introduce IQ imbalance. To this end, the time domain (TD) transmit signal  $x_{\text{TD}}$  at the transmitter and receive signal  $y_{\text{TD}}$  at the receiver are interfered by their respective complex conjugates, as shown in Fig. 17 for the simplified block diagram. Therein,  $\alpha_i$  and  $\beta_i$ ,  $i \in \{t, r\}$ , represent the weighting factors at either the transmitter or the receiver. Equipped with this model and

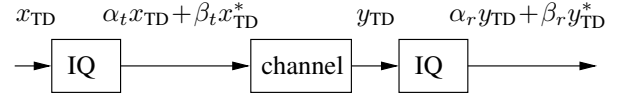


Fig. 17: Simplified block diagram for illustration of incorporating IQ imbalance at both the transmitter and the receiver.

assuming  $\mathbf{x}$  the transmit signal vector, the noise-free receive signal vector  $\hat{\mathbf{x}}$  after equalization is derived in [18], [19] and given for OFDM transmission by

$$\hat{\mathbf{x}} = \alpha_r \alpha_t \mathbf{x} + \beta_r \beta_t^* \mathbf{G} \mathbf{H}^\# \mathbf{x} + \alpha_r \beta_t \mathbf{x}^\# + \beta_r \alpha_t^* \mathbf{G} \mathbf{H}^\# \mathbf{x}^\# \quad (8)$$

and for SC-FDE transmission by

$$\hat{\mathbf{x}} = \alpha_r \alpha_t \mathbf{x} + \beta_r \beta_t^* \mathbf{F}^H \mathbf{G} \mathbf{H}^\# \mathbf{F} \mathbf{x} + \alpha_r \beta_t \mathbf{x}^* + \beta_r \alpha_t^* \mathbf{F}^H \mathbf{G} \mathbf{H}^\# \mathbf{F} \mathbf{x}^* . \quad (9)$$

Here,  $\mathbf{H}$  and  $\mathbf{G}$  denote the diagonal channel matrix and the equalization matrix, respectively.  $\mathbf{F}$  represents the discrete Fourier transform (DFT) matrix used to perform the FFT/IFFT operations. The mirror and conjugate operator  $(\cdot)^\#$  has been defined in [18]. For an arbitrary vector  $\mathbf{a}$  of length  $N$ , the  $k$ th element of  $\mathbf{a}^\#$  is given by  $a^\#(k) = a^*(N-k)$ . Similarly, the  $(k, \ell)$ th element of  $\mathbf{A}^\#$  reads  $a^\#(k, \ell) = a^*(N-k, N-\ell)$  with  $\mathbf{A}$  denoting an arbitrary square matrix of size  $N \times N$ . It can be observed in (8) that the interference comes from  $\mathbf{x}^\#$  for OFDM, whereas it originates from  $\mathbf{x}^*$  for SC-FDE as indicated by (9). Moreover, the second interference term can be interpreted as the interference signal transmitted over the mirrored and conjugated channel  $\mathbf{H}^\#$  but equalized with respect to the original channel [17]. As a result, a high gain subcarrier may interfere on a low gain subcarrier located at the other side of the spectrum, thus totally corrupting the signal detection there.

For performance evaluation with IQ imbalance, both uncoded BER and coded FER for OFDM and SC-FDE are presented in Fig. 18 and Fig. 19, respectively. Different values of amplitude and phase mismatches are considered. It can be observed that SC-FDE is more robust against IQ imbalance than OFDM. This is because the matrix  $\mathbf{G} \mathbf{H}^\#$  is left and right multiplied with  $\mathbf{F}^H$  and  $\mathbf{F}$  in the second interference term for SC-FDE in (9). Via this operation, the interference coming from all symbols is averaged leading to mitigated performance degradation. However, SC-FDE suffers from a raised error rate at high SNR due to the fact that the MMSE equalizer is designed irrespective of the interference caused by IQ imbalance. As a consequence, the interference is essentially amplified with growing SNR until convergence to that for a zero-forcing (ZF) equalizer. In coded systems, the impairment from IQ imbalance is compensated dramatically by channel coding for both OFDM and SC-FDE transmissions. For example, even a phase mismatch of  $\Delta\phi = 10^\circ$  approaches the ideal case within 1 dB, although a raised FER is observed at high SNR in this case.

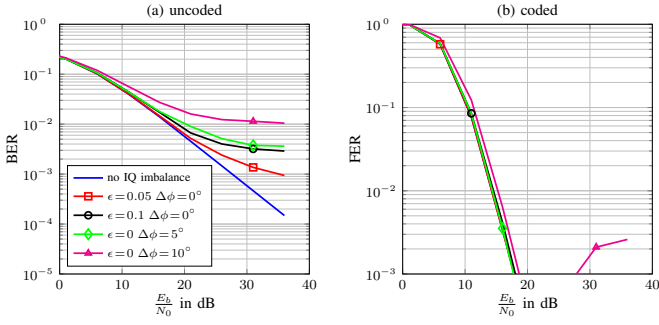


Fig. 18: Error rate for OFDM with IQ imbalance of different mismatch values, (a) for uncoded BER and (b) for coded FER.

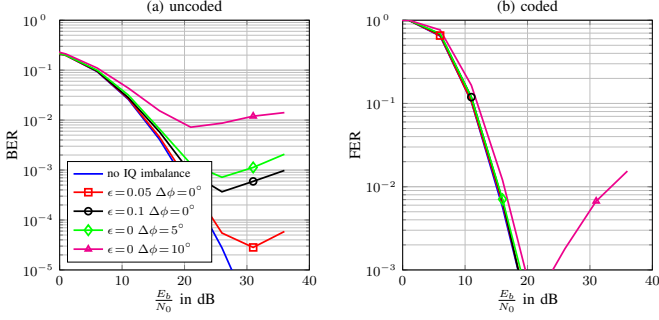


Fig. 19: Error rate for SC-FDE with IQ imbalance of different mismatch values, (a) for uncoded BER and (b) for coded FER.

## VI. ADC RESOLUTION

In digital communication systems, ADC and digital-to-analog converter (DAC) with finite resolution are applied at the receiver and transmitter, respectively. On one hand, using more quantization bits offers higher precision for signal conversion between the digital and analog domains. On the other hand, the power dissipation of ADC scales exponentially with the resolution [20], i.e., adding one more quantization bit doubles the energy cost of the ADC. To this end, investigations are required for practical ADC designs with less quantization while preserving the system performance. This issue is especially important for communications at mmWave range because large number of antennas as well as RF chains is usually assumed for digital beamforming in this case, leading to prohibitive hardware energy cost with high-resolution ADC/DACs. One solution to loose the constraint is performing hybrid beamforming with much less RF chains such that the number of required ADC/DACs is reduced significantly [21]. Alternatively, low-resolution ADC/DACs can be applied while losing not much precision. Corresponding investigations are related to, e.g., [22], [23], [24]. In this paper, we focus on the single-stream transmission scenario [6] requiring one ADC with finite resolution at the receiver and study the impact of employing different number of quantization bits on the system performance. Extension to MIMO setup with multiple RF chains and impact of ADC are considered as future work.

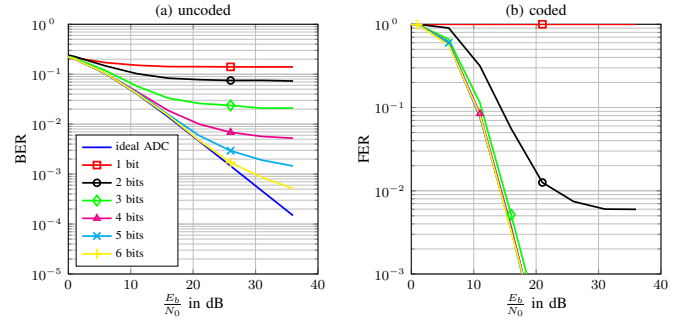


Fig. 20: Error rate for OFDM with ADC of different quantization bits, (a) for uncoded BER and (b) for coded FER.

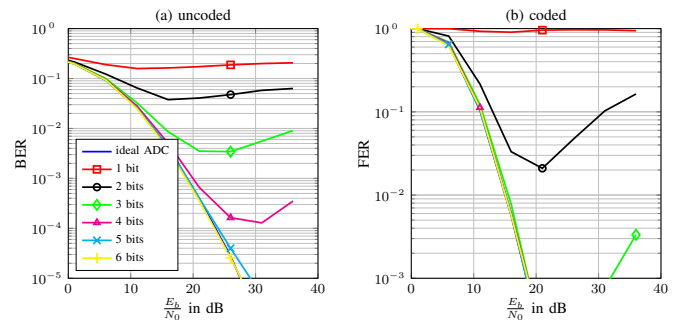


Fig. 21: Error rate for SC-FDE with ADC of different quantization bits, (a) for uncoded BER and (b) for coded FER.

In Fig. 20 and Fig. 21, both uncoded BER and coded FER for OFDM and SC-FDE using ADC with finite resolution are presented, respectively. For these results, an ideal DAC is assumed. Uniform quantization is used for the real part and imaginary part of the signal separately. To avoid clipping, the quantizer threshold is set to the peak value with the implementation of automatic gain control (AGC). As can be observed, SC-FDE performs much more robustly against ADC imprecision over OFDM for uncoded transmissions due to lower PAPR, which results in smaller quantization steps with higher precision. Specifically, 5 quantization bits are sufficient to reach the ideal case for SC-FDE whereas even 6 quantization bits for OFDM result in an error floor. Additionally, a raised BER is observed for SC-FDE until 4 quantization bits due to similar reasons for IQ imbalance in the previous section, i.e., the quantization noise is not considered in the MMSE equalizer. In case of coded transmission an ADC resolution of 3 bits is sufficient for OFDM to achieve ideal performance. For 2 quantization bits an error floor is observed at  $\text{FER} = 6 \cdot 10^{-3}$ . Similar, for SC-FDE 3 bits are sufficient to achieve ideal performance and even with 2 bits an improved performance at low to medium SNR compared to OFDM is achieved. However, for both cases an increase of the FER is observed for large SNR. This effect is due to the fact, in case of SC-FDE the quantization noise is uniformly distributed leading to inexact LLR calculation as it does not meet the assumption of Gaussian noise variance for the symbol

demapper. In contrast, for OFDM the effective quantization noise follows a Gaussian distribution due to FFT operation.

## VII. CONCLUSION

In the paper, the impact of hardware impairments from phase noise (PN), non-linear power amplifiers (NPA), IQ imbalance and analog-to-digital converter (ADC) are analyzed and compared for both OFDM and SC-FDE transmissions in an outdoor urban mmWave environment. Numerical results indicate that OFDM is slightly more robust against PN than SC-FDE. On the other hand, SC-FDE is more immune to imprecisions caused by NPA, IQ imbalance and ADC resolution. It has also been shown that although channel coding compensates the less robustness of OFDM to a large extent, SC-FDE still outperforms OFDM even in some coded cases.

## REFERENCES

- [1] C.-S. Choi, Y. Shoji, H. Harada, R. Funada, S. Kato, K. Maruhashi, I. Toyoda, and K. Takahashi, "RF Impairment Models for 60GHz-band SYS/PHY Simulation," Tech. Rep., IEEE 802.15-06-0477-01-003c, Nov. 2006.
- [2] R. Gomes, Z. Al-Daher, A. Hammoudeh, R. Caldeirinha, and T. Fernandes, "Performance and Evaluation of OFDM and SC-FDE over an AWGN Propagation Channel under RF Impairments using Simulink at 60GHz," in *Loughborough Antennas and Propagation Conference (LAPC'14)*, Loughborough, England, Nov. 2014.
- [3] M. Lei, I. Lakkis, C.-S. Sum, T. Baykas, J.-Y. Wang, M. A. Rahman, R. Kimura, R. Funada, Y. Shoji, H. Harada, and S. Kato, "Hardware Impairments on LDPC Coded SC-FDE and OFDM in Multi-Gbps WPAN (IEEE 802.15.3c)," in *IEEE Wireless Communications and Networking Conference (WCNC'08)*, Las Vegas, NV, USA, Apr. 2008.
- [4] T. A. Thomas, H. C. Nguyen, G. R. MacCartney, and T. S. Rappaport, "3D mmWave Channel Model Proposal," in *IEEE 80th Vehicular Technology Conference (VTC'14-Fall)*, Vancouver, Canada, Sept. 2014.
- [5] T. Bai, A. Alkhatieb, and R. W. Heath, "Coverage and Capacity of Millimeter-Wave Cellular Networks," *IEEE Communications Magazine*, vol. 52, no. 9, pp. 70–77, Sept. 2014.
- [6] M. Wu, D. Wübben, A. Dekorsy, P. Baracca, V. Braun, and H. Halbauer, "On OFDM and SC-FDE Transmissions in Millimeter Wave Channels with Beamforming," in *IEEE 83rd Vehicular Technology Conference (VTC'16-Spring)*, Nanjing, China, May 2016.
- [7] D. Falconer, S. Ariyavisitakul, A. Benyamin-Seeyar, and B. Eidson, "Frequency Domain Equalization for Single-Carrier Broadband Wireless Systems," *IEEE Communications Magazine*, vol. 40, no. 4, pp. 58–66, Apr. 2002.
- [8] EU FP7 METIS, "Deliverable D2.3: Components of a New Air Interface - Building Blocks and Performance," Apr. 2014.
- [9] E. Perahia, "IEEE P802.11 Wireless LANs TGad Evaluation Methodology," Tech. Rep., IEEE 802.11-09/0296r16, Jan. 2009.
- [10] Y.-C. Liao and K.-C. Chen, "Estimation of Stationary Phase Noise by the Autocorrelation of the ICI Weighting Function in OFDM Systems," *IEEE Transactions on Wireless Communications*, vol. 5, no. 12, pp. 3370–3374, Dec. 2006.
- [11] A. Ischaque and G. Ascheid, "On the Sensitivity of SMT Systems to Oscillator Phase Noise over Doubly-Selective Channels," in *IEEE Wireless Communications and Networking Conference (WCNC'15)*, New Orleans, LA, USA, Mar. 2015.
- [12] J. L. Zamorano, J. Nsenga, W. Van Thillo, A. Bourdoux, and F. Horlin, "Impact of Phase Noise on OFDM and SC-CP," in *IEEE Global Telecommunications Conference (GLOBECOM'07)*, Washington, DC, USA, Nov. 2007.
- [13] M. Honkanen and S.-G. Haggman, "New Aspects on Nonlinear Power Amplifier Modeling in Radio Communication System Simulations," in *IEEE International Symposium on Personal, Indoor, and Mobile Communications (PIMRC'97)*, Helsinki, Finland, Sept. 1997.
- [14] A. Maltsev, A. Lomayev, and R. Maslennikov, "Comparison of Power Amplifier Non-linearity Impact on 60 GHz Single Carrier and OFDM Systems," in *7th Consumer Communications and Networking Conference (CCNC'10)*, Las Vegas, NV, USA, Jan. 2010.
- [15] M. Senst and G. Ascheid, "Optimal Output Back-Off in OFDM Systems with Nonlinear Power Amplifiers," in *IEEE International Conference on Communications (ICC'09)*, Baltimore, MD, USA, Jun. 2009.
- [16] B. Razavi, *RF Microelectronics*, Prentice Hall, second edition, 2011.
- [17] F. Horlin and A. Bourdoux, "Comparision of the Sensitivity of OFDM and SC-FDE to CFO, SCO and IQ Imbalance," in *3rd International Symposium on Communications, Control and Signal Processing (IS-CCSP'08)*, St. Julians, Malta, Mar. 2008.
- [18] A. Tarighat and A. H. Sayed, "Joint Compensation of Transmitter and Receiver Impairments in OFDM Systems," *IEEE Transactions on Wireless Communications*, vol. 6, no. 1, pp. 240–247, Jan. 2007.
- [19] S. Narayanan, B. Narasimhan, and N. Al-Dhahir, "Baseband Estimation and Compensation of Joint TX/RX IQ Imbalance in SC-FDE Transceivers," in *43rd Annual Conference on Information Sciences and Systems (CISS'09)*, Baltimore, MD, USA, Mar. 2009.
- [20] H.-S. Lee and C. G. Sodini, "Analog-to-Digital Converters: Digitizing the Analog World," *IEEE Proceedings*, vol. 96, no. 2, pp. 323–334, Feb. 2008.
- [21] O. El-Ayach, S. Rajagopal, S. Abu-Surra, Z. Pi, and R. W. Heath, "Spatially Sparse Precoding in Millimeter Wave MIMO Systems," *IEEE Transactions on Wireless Communications*, vol. 13, no. 3, pp. 1499–1513, Mar. 2014.
- [22] J. Singh, O. Dabeer, and U. Madhoo, "On the Limits of Communication with Low-Precision Analog-to-Digital Conversion at the Receiver," *IEEE Transactions on Communications*, vol. 57, no. 12, pp. 3629–3639, Dec. 2009.
- [23] N. Belli, N. Benvenuto, F. Boccardi, H. Halbauer, and P. Baracca, "Fully-Digital Millimeter-Wave Receivers with Low-Resolution Analog-to-Digital Converters," in *IEEE Global Telecommunications Conference (GLOBECOM'13) Workshops*, Atlanta, GA, USA, Dec. 2013.
- [24] J. Mo and R. W. Heath, "High SNR Capacity of Millimeter Wave MIMO Systems with One-Bit Quantization," in *Information Theory and Applications Workshop (ITA'14)*, San Diego, CA, USA, Feb. 2014.